Nanophononic thin-film filters and mirrors studied by picosecond ultrasonics

N. D. Lanzillotti-Kimura,[1,2,a)] B. Perrin,[1] A. Fainstein,[2] B. Jusserand,[1] and A. Lemaître[3]
[1]*Institut des NanoSciences de Paris, UMR 7588 CNRS—Université Pierre et Marie Curie, 75015 Paris, France*
[2]*Centro Atómico Bariloche & Instituto Balseiro, CNEA, S. C. de Bariloche, 8400 Río Negro, Argentina*
[3]*Laboratoire de Photonique et de Nanostructures, CNRS, 91460 Marcoussis, France*

(Received 3 December 2009; accepted 29 December 2009; published online 1 February 2010)

Optimized acoustic phonon thin-film filters are studied by picosecond ultrasonics. A broadband mirror and a color filter based on aperiodic multilayers were optimized to work in the subterahertz range, and grown by molecular beam epitaxy. Time resolved differential optical reflectivity experiments were performed with pump and probe pulses incident on opposite sides of the substrate. We provide broadband transmission curves for the phonon devices. The results are in good agreement with standard transfer matrix method simulations. In addition, we analyze the effects of the free surface and the influence of an Al capping layer on the response of the aperiodic devices.
© *2010 American Institute of Physics*. [doi:10.1063/1.3295701]

The engineering of devices to manipulate and control acoustic vibrations in solids is a main issue in the development of applications in nanophononics.[1–8] Inspired by previous concepts in photonics and electronics,[9] several thin-film filters in the terahertz (THz) range have been recently proposed.[3,6,10] By engineering the thickness distribution in aperiodic multilayers, it is possible to conceive structures with tailored phononic transmission properties.[3,6] For applications in the gigahertz (GHz)-THz frequency range, the typical layer thickness must be in the nanometer scale and the interfaces must be atomically flat. The development of epitaxial growth techniques have reached the standards for this kind of hypersound applications.[3,6,11] However, the characterization and evaluation of such devices was limited by the availability of experimental setups to perform hyperacoustic transmission experiments similar to those used in lower frequency acoustics.[12] Recently, some schemes based on picosecond ultrasonics[13,14] have been demonstrated to probe the transmission spectrum through a nanowave device.[4,5] Phonon mirrors and acoustic nanocavities have been characterized in this way using picosecond ultrasonics and metallic transducers.[4] In this letter we present the direct demonstration of optimized thin-film hypersound filters through experimental phononic transmission results in the sub-THz range. Two optimized devices based on GaAs/AlAs multilayers were grown by molecular beam epitaxy: a broadband mirror and a color filter. These devices were characterized by pump-probe time resolved reflectivity experiments. We compare the experimental results with simulations performed using an implementation of the standard transfer matrix method and taking into account the appropriate acoustic boundary conditions.[8] The role of the sample/air interface on the response of the device is also discussed.

Optical thin-film filters are usually characterized by reflection/transmission experiments. These measurements require both light sources and detectors. In GHz-THz hyperacoustics, the lack of versatile generators and detectors represents one of the main limitations in the study of ultrahigh frequency sound propagation. In recent years great efforts have been made in order to develop tools and strategies to generate and detect acoustic phonons, and to study their propagation over long distances. Particularly, it has been shown that it is possible to use metallic thin-films as transducers to generate and detect broadband coherent acoustic phonons in the sub-THz range, and use crystalline substrates as the propagating media.[4]

We designed and studied two thin-film filters. The samples consist of GaAs/AlAs aperiodic multilayers on a GaAs substrate (panel a, Fig. 1). In order to simulate the acoustic reflectivity, we used a transfer matrix method.[8] Since in actual nanophononics applications filters should be coupled to other components through solid media (to allow energy transport), during the design and optimization stages we considered that the devices are embedded in a GaAs medium. The first device under study is a broadband mirror (BM). A BM presents a high reflectivity over a band much larger than the typical widths of the superlattice minigaps.[15]

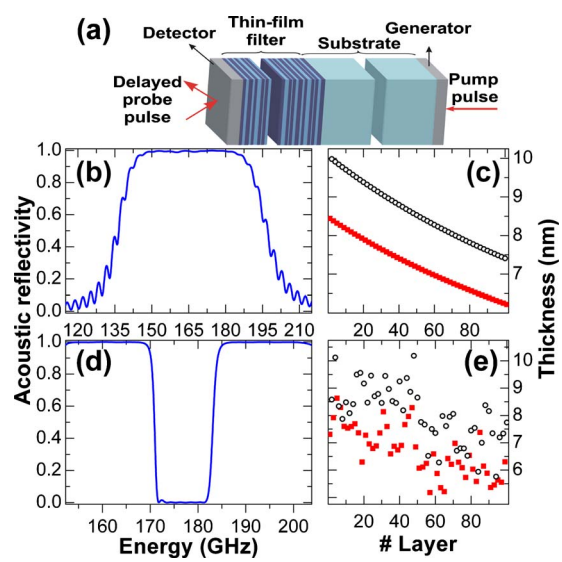

FIG. 1. (Color online) Panel a: schematics of the sample and experimental phononic transmission configuration. Panel b (d): calculated acoustic reflectivity for the optimized broadband mirror (color filter) sample. Panel c (e): thickness distribution in the optimized broadband mirror (color filter).

[a)]Electronic mail: kimura@cab.cnea.gov.ar.

 © 2010 American Institute of Physics

Downloaded 02 Feb 2010 to 200.0.233.51. Redistribution subject to AIP license or copyright; see http://apl.aip.org/apl/copyright.jsp

A BM can be conceived as a superposition of phononic distributed Bragg reflectors shifted in energy, giving rise to stopbands up to five times larger than those present in optimized periodic structures. We designed this device as a concatenation of (GaAs, AlAs) $(\lambda/4,\lambda/4)$ bilayers, where λ is the acoustic wavelength. This thickness relation maximizes the first acoustic phonon minigap at the Brillouin zone edge.[16] The designed BM consists of 50 GaAs/AlAs bilayers, with thicknesses ranging from 6.22 to 9.98 nm. We set a gradient of 1 GHz/bilayer, resulting in bilayers centered between 140 and 190 GHz. Panels b and c in Fig. 1 present the calculated acoustic reflectivity and layer thickness distribution for this device. Full squares (empty circles) correspond to GaAs (AlAs) layers. The reflectivity curve is characterized by a high-reflectivity band (above 98%) of ~40 GHz, centered at 165 GHz. This can be compared with the 8.75 GHz obtained with a periodic 50 bilayers $(\lambda/4,\lambda/4)$ mirror.

The second device under study is a color filter (CF). A CF is characterized by having a very high transmission for a defined frequency band, and, at the same time, by being highly reflective to adjacent frequencies. The design of the acoustic thin-film CF was performed in a two step optimization process as described in Ref. 6, using a Nelder–Mead downhill simplex algorithm.[17] For the optimization of these filters two shifted 25 periods (GaAs, AlAs) $(\lambda/4,\lambda/4)$ SLs were used as seeds. Panels d and e of Fig. 1 present the optimized acoustic reflectivity and the layer thickness distribution of the CF. The thicknesses range from 5.17 to 10.18 nm. The CF presents an operating band between ~152.3 and 203.8 GHz. The pass band width is ~12.25 GHz, and presents a transmission higher than 99.985%, while the blocked bands present a reflectivity higher than 98%.

Both samples were grown on (001) GaAs double side polished substrates using molecular beam epitaxy (MBE). High resolution x-ray diffraction (HRXRD) was used for structural characterization, obtaining a good agreement with simulations performed using nominal thickness values.

We used a femtosecond mode locked Ti-Sapphire laser providing 80 fs pulses in the near-IR range, with a 80 MHz repetition rate to perform pump-probe coherent phonon generation experiments in acoustic transmission geometry.[4] The pump was modulated at 2 MHz and the probe was detected using a lock-in amplifier. Both beams were focused onto 60 μm spots, on different sides of the sample. Typical energies were a few nanojoules/pulse for the pump, and approximately ten times less energy for the probe. Two aluminum thin-films of ≈30 nm were grown on the sample and substrate sides to act as broadband coherent acoustic phonon detector and generator, respectively (panel a, Fig. 1). The pump pulse was focused on the Al thin-film generator (substrate side), delivering a phonon pulse with frequency components up to 200 GHz.[18] Due to nonlinear distortions, higher frequencies may appear after propagation through the ~350 μm substrate.[19] The probe beam is focused on the second Al thin-film (detector, sample side). The phonons that traverse the acoustic device modulate the optical properties of the detector, changing its reflectivity. The intensity of the reflected probe beam is then measured as a function of the time delay between pump and probe pulses. A time scan of 750 ps delay between pump and probe was performed. By Fourier transforming the time resolved reflectivity signal, we can determine which frequencies actually reach the second metallic transducer, evaluating the transmission characteristics of the aperiodic devices. The thickness of these Al light-hypersound transducers is optimized to reduce the acoustic attenuation in the metal and to maximize the optical attenuation in order to avoid direct excitation of the substrate and detection within the sample. We worked at 15 K to minimize the acoustic attenuation within the GaAs substrate during propagation between the generator and the detector. The time dependent reflectivity curves were measured using a Sagnac interferometer,[20–22] which allowed us to recover the changes in reflectivity mainly due to the metallic surface displacement. Furthermore, because of the high light absorption coefficient of the Al film, we can consider that the only contributions to the change in the reflectivity come from the metallic thin-film, neglecting any possible change in the optical constants of the aperiodic device. Calculations were performed assuming a "white" strain wavepacket coming from the substrate and evaluating directly the surface displacement of the metallic detector. The broadening effects introduced by a time window of 750 ps were taken into account.

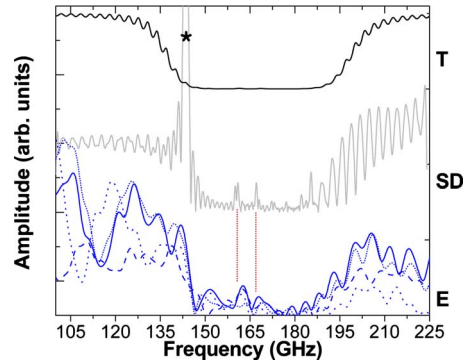

FIG. 2. (Color online) Acoustic phonon transmission through the broadband mirror. SD stands for the calculated surface displacement. E indicates the experimental transmission spectra, the different curves correspond to different laser powers. The vertical lines indicate localized modes in the structure, while the asterisk (*) identifies the confined mode in the aluminum thin film. T is the calculated transmission spectrum of the device embedded in a GaAs matrix.

The experimental results and simulations for the BM are presented in Fig. 2. The curve indicated with E corresponding to the experimental spectrum (thick line) is compared with the calculated surface displacement (SD), evaluated for the actual structure including the Al film and considering a free surface. The theoretical transmission (T) of the BM in a GaAs medium is also included in the upper part of the figure. The theoretical transmission curve T is characterized by a large band gap and lateral oscillations. The calculated SD curve, on the other hand displays, in addition to a general behavior similar to that shown in T, a peak at 143GHz, which is indicated with an asterisk (*). This peak corresponds to a localized mode in the Al thin-film. Moreover, in the high reflectivity band, two additional modes can be observed. These peaks are associated to confined modes between the surface and zones in the structure having a high local reflectivity band in these energies. The experimental curve shows a well defined high reflectivity band. There are, however, some low intensity features within this band that can be related to the confined modes (vertical lines). The Al-localized mode (*) can also be observed in the experimental spectra, but with a different intensity with respect to the other fea-

Downloaded 02 Feb 2010 to 200.0.233.51. Redistribution subject to AIP license or copyright; see http://apl.aip.org/apl/copyright.jsp

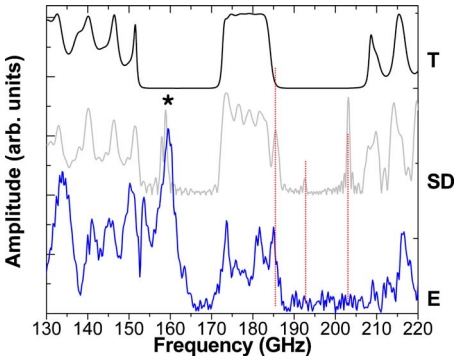

FIG. 3. (Color online) Acoustic phonon transmission through the optimized color filter. SD stands for the calculated surface displacement. E indicates the experimental transmission spectrum. The vertical lines indicate localized modes in the structure, while the asterisk (*) identifies the confined mode in the aluminum thin film. T is the calculated transmission spectrum of the device embedded in a GaAs matrix.

tures. This can be originated by losses due to electron-phonon interactions in the Al layer, which result enhanced due to the acoustic confinement in the Al layer. From the position of the peak (*) we determined that the actual Al thickness is ~31.5 nm, close to the nominal value of 30 nm. The rest of the features are practically independent of the Al layer thickness. Lateral oscillations in the experimental curve are partially reproduced by the simulations. It must be noted that the experimental spectra present an intensity modulation due to the incident acoustic pulse, which is not white. We have verified this from spectra taken with different pump powers, and thus, different incident spectra, because of nonlinear effects acting on the propagating pulse (dotted lines in Fig. 2).

The experimental results and simulations for the CF are presented in Fig. 3. In the lower part, the measured transmission spectrum is shown with the thick line (E). The dotted line corresponds to the simulation of the surface displacement (SD) taking into account effects due to the actual sample with Al transducers. The calculated transmission spectrum (T) of the device embedded in an infinite GaAs matrix is included to identify the high/low reflectivity bands. From the experimental curve it can be noted that: (i) the passband of the CF is well defined. (ii) the two high reflectivity bands are also clearly defined, except for the presence of a strong peak indicated with an asterisk (*). (iii) The mode identified with an asterisk corresponds to a localized mode in the Al film (detector side). The difference in linewidth of this mode can be attributed to acoustic absorption in the metal not taken into account in the simulations. (iv) There are side oscillations that are partially reproduced by the simulations. (v) Oscillations in the passband due to surface effects are observed in the experiments and partially reproduced in the SD curve. Again, the different amplitude relation between peaks in SD and E can be also associated to the incident spectrum which is not perfectly white. Since the incident spectrum is basically broadband but modulated, it is not possible to directly evaluate the contrast between the low and high-reflectivity bands of the nanowave devices.

The agreement between the experiments and the surface displacement simulations indicates that the devices perform according the their original conception. The results also demonstrate that, in the design of phonon thin-film filters, it is essential to consider in the optimization process the full medium in which the devices are embedded.

To summarize, we have presented two devices designed using $(\lambda/4,\lambda/4)$ SLs as seeds, which maximize the width of the first acoustic minigap at the Brillouin zone edge.[15] The broadband mirror and the color filter were optimized to work in the 150–220 GHz range adapted to generation and detection using Al films. The growth of these superstructures was done by MBE. We have performed hypersonic transmission experiments on such optimized thin-film devices. With highly promising results for future nanophononics applications, these devices were able to filter a specific band (color filter), and to reject a broad band (optimized mirror). The importance of the presence of a free surface and the capping layer has been evidenced. Taking into account the presence of the metallic layer and appropriate acoustic boundary conditions, the behavior of these devices in the specific experimental conditions used was qualitatively reproduced by the simulations.

The authors acknowledge O. Mauguin and L. Largeau for the HRXRD characterization of the samples, and R. Gohier for the sample preparation for pump probe experiments. N.D.L.K. acknowledges support from Fundación YPF (Argentina) and Programme Alban through Scholarship No. E06D103192AR. A.F. also acknowledges support from ANPCyT through Grant No. PICT2004 25316.

[1] A. A. Balandin, J. Nanosci. Nanotechnol. **5**, 1015 (2005).
[2] M. M. de Lima, R. Hey, P. V. Santos, and A. Cantarero, Phys. Rev. Lett. **94**, 126805 (2005).
[3] N. D. Lanzillotti-Kimura, A. Fainstein, A. Lemaître, and B. Jusserand, Appl. Phys. Lett. **88**, 083113 (2006).
[4] A. Huynh, N. D. Lanzillotti-Kimura, B. Jusserand, B. Perrin, A. Fainstein, M. F. Pascual Winter, E. Perónne, and A. Lemaître, Phys. Rev. Lett. **97**, 115502 (2006).
[5] K.-H. Lin, C.-F. Chang, C.-C. Pan, J.-I. Chyi, S. Keller, U. Mishra, S. P. DenBaars, and C.-K. Sun, Appl. Phys. Lett. **89**, 143103 (2006).
[6] N. D. Lanzillotti-Kimura, A. Fainstein, B. Jusserand, O. Mauguin, L. Largeau, and A. Lemaître, Phys. Rev. B **76**, 174301 (2007).
[7] E. S. Landry, M. I. Hussein, and A. J. H. McGaughey, Phys. Rev. B **77**, 184302 (2008).
[8] N. D. Lanzillotti-Kimura, A. Fainstein, C. A. Balseiro, and B. Jusserand, Phys. Rev. B **75**, 024301 (2007).
[9] P. Baumeister, J. Opt. Soc. Am. **48**, 955 (1958).
[10] M. Trigo, A. Bruchhausen, A. Fainstein, B. Jusserand, and V. Thierry-Mieg, Phys. Rev. Lett. **89**, 227402 (2002); J. M. Worlock and M. L. Roukes, Nature (London) **421**, 802 (2003).
[11] A. Soukiassian, W. Tian, D. A. Tenne, X. X. Xi, D. G. Schlom, N. D. Lanzillotti-Kimura, A. Bruchhausen, A. Fainstein, H. P. Sun, X. Pan, A. Cross, and A. Cantarero, Appl. Phys. Lett. **90**, 042909 (2007).
[12] H. Sanchis-Alepuz, Y. A. Kosevich, and J. Sanchez-Dehesa, Phys. Rev. Lett. **98**, 134301 (2007).
[13] C. Thomsen, H. T. Grahn, H. J. Maris, and J. Tauc, Phys. Rev. B **34**, 4129 (1986).
[14] G. A. Antonelli, B. Perrin, B. C. Daly, and D. G. Cahill, MRS Bull. **31**, 607 (2006).
[15] B. Jusserand and M. Cardona, in *Light Scattering in Solids V*, edited by M. Cardona and G. Güntherodt (Springer, New York, 1989), p. 49.
[16] For the same energy, the minigap is twice larger than the minigap corresponding to the equivalent $(3\lambda/4,\lambda/4)$ structure as indicated in Ref. 15. In addition, the total thickness of the sample is reduced.
[17] J. A. Nelder and R. Mead, Comput. J. **7**, 308 (1965).
[18] A. Huynh, B. Perrin, N. D. Lanzillotti-Kimura, B. Jusserand, A. Fainstein, and A. Lemaitre, Phys. Rev. B **78**, 233302 (2008).
[19] E. Péronne and B. Perrin, Ultrasonics **44**, e1203 (2006).
[20] B. Perrin, B. Bonello, J.-C. Jeannet, and E. Romatet, Prog. Nat. Sci. **S6**, 444 (1996).
[21] J.-Y. Duquesne and B. Perrin, Phys. Rev. B **68**, 134205 (2003).
[22] T. Tachizaki, T. Muroya, O. Matsuda, Y. Sugawara, D. H. Hurley, and O. B. Wright, Rev. Sci. Instrum. **77**, 043713 (2006).

Downloaded 02 Feb 2010 to 200.0.233.51. Redistribution subject to AIP license or copyright; see http://apl.aip.org/apl/copyright.jsp